

Determination of Fe³⁺ in Water Samples by Reduced Schiff Base Ligand

Sunti DOUNGCHANDENG¹, Nuttapon APIRATIKUL¹, Itthipol SUNGWIEWWONG¹,
Piyarat SRIVILAI¹ and Pan TONGRAUNG^{1*}

Received: 14 November 2024

Revised: 7 December 2024

Accepted: 12 December 2024

ABSTRACT

This research presents the development of a method for the quantification of Fe³⁺ using a reduced Schiff base ligand, which was synthesized via a simple two-step process with a high yield of 84%. The quantification of Fe³⁺ was analyzed using UV-Visible spectrophotometry. The selective binding of ligand with various cations (Fe³⁺, Cr³⁺, Pb²⁺, Co²⁺, Cu²⁺, Zn²⁺, Cd²⁺, Hg²⁺, Mn²⁺, Ni²⁺, Fe²⁺, Mg²⁺, Ag⁺, Na⁺, K⁺) was investigated. The results revealed that the reduced Schiff base ligand specifically formed a complex with Fe³⁺, indicated by a new absorption peak in the 350–400 nm range due to ligand-to-metal charge transfer (LMCT). In contrast, other cations induced no significant spectral changes. Quantitative studies of Fe³⁺ showed that the absorbance at 380 nm increased linearly with Fe³⁺ concentration, displaying a correlation coefficient (R^2) of 0.9994 within the Fe³⁺ concentration range of 2.00×10^{-6} to 1.00×10^{-3} M. The method exhibited a limit of detection (LOD) of 1.22×10^{-6} M and a limit of quantification (LOQ) of 2.03×10^{-5} M. The reduced Schiff base ligand was successfully applied for Fe³⁺ quantification in real water samples, corresponding to the results obtained by inductively coupled plasma optical emission spectroscopy (ICP-OES).

Keywords: Reduced Schiff base ligand, Sensor, Fe³⁺, Water samples.

¹ Department of Chemistry, Faculty of Science, Srinakharinwirot University, Bangkok 10110, Thailand

* Corresponding author, email: pan@g.swu.ac.th

Introduction

Iron is an important element in the human body. It is extremely important for the metabolic process which plays an important role in physiology. Iron displays a role in many chemical and biological processes, such as metabolic processes, oxygen transport respiration and electron transfer [1-4]. Quantification of iron is important for human health. Accumulation of iron in the body can result in kidney and liver damage, including abnormalities of vital organs which can cause cancer, hemochromatosis, and symptoms of hepatitis [5-8]. Iron deficiency prevents the synthesis of certain enzymes and proteins which can affect oxygen transport, causing many diseases, including cell metabolism problems and anemia [9-11]. The average amount of iron that a person should receive is approximately 3.8 grams for men and 2.3 grams for women [12-13].

Water is an essential resource for all living organisms, especially humans. Wastewater from industrial factories lacking effective waste control and treatment systems, as well as from agriculture and household activities, often flows into water sources, contaminating them with heavy metals. Iron is one of metals that contaminates water sources, causing in water pollution. Therefore, monitoring and assessing the quality of water resources, including iron content, is critically important.

From the importance of iron mentioned above, accurate analysis of iron content in various samples, especially water samples, is therefore very important. Numerous methods have been developed for iron analysis in many samples [14-19]. There are several techniques that can be used to analyzed iron with high sensitivity, good accuracy and precision. However, these techniques are usually large and expensive, and require an analytical person with experience and expertise in using tools. Moreover, some techniques require complicated sample preparation before analysis.

Over the past decades, many researchers have been interested in designing and synthesizing chemosensors to simply measure heavy metals with good specificity and high sensitivity. Schiff base groups are frequently incorporated into chemosensor designs due to their unique properties; 1) being both a receiver and a transmitter, 2) various precursors for synthesis and easy to find, and 3) easy to synthesize and purify with high productivity and low costs [20-23]. Schiff base can bind to metal ions including iron ions and change the optical signal. Researchers are therefore competing to design synthetic chemosensors that can detect heavy metals with a low LOD and a wide measurement range [24] with high efficiency [25]. Although these chemosensors have various advantages mentioned above, but they do not selectively bind to only one type of metal ion. They rather bind with more than one type of metal ion [25-28].

Longyan Wang et al. [11] reported a Schiff base probe obtained by the synthesis of diketopyrrolopyrrole and *p*-methoxyaniline which can be used to measure Fe^{3+} and Al^{3+} with decreased fluorescence signal when binding to Fe^{3+} and increased signal when binding to Al^{3+} . Min Zhang et al. [29] reported a Schiff base probe, synthesized from 2-hydroxy-1-naphthaldehyde and 5-aminosalicylic acid, that can measure Fe^{3+} , Al^{3+} , Cr^{3+} , and Cu^{2+} . There was an increase in the fluorescent signal when binding with Al^{3+} , and a decrease in the fluorescent signal when binding with Fe^{3+} . Changes of color of the solution were observed differently when binding with Cr^{3+} and Cu^{2+} .

The synthesis of chemosensors that selectively bind to Fe^{3+} by altering the fluorescent signal has been reported. However, there were many complicated synthesis steps that resulted in low yield. Most importantly, they used solvents that were not environmentally friendly [30-32]. Li, Z. et al. [33] synthesized

a chemosensor that selectively bound to Fe^{3+} in a 'turn on' manner with a four-step synthesis process using DMF and CHCl_3 as solvents. Ruiping, W. et al. [34] also synthesized a chemosensor that specifically bound to Fe^{3+} , but pyridine was used as a solvent with 3 steps of synthesis, resulting in low yield. Changing the chemosensor to reduced Schiff base ligand allowed it to selectively bind to Fe^{3+} . It has been reported that synthesized Schiff base - naphthalene-2-ol [35] can selectively bind to Cu^{2+} , but when reducing Schiff base was made, it was found that it could selectively bind to only Fe^{3+} . Importantly, the synthesis was easy with high yield. When binding to Fe^{3+} , the fluorescent signal was suppressed, and spectral changes occurred due to electron transfer from ligand to metal ion (LMCT). In addition, this research group performed a preliminary Fe^{3+} binding study with the fluorescence signal decreasing with addition of Fe^{3+} [36]. However, reduced Schiff base has not been used as a detector to quantify Fe^{3+} in real samples.

Given the critical role of Fe^{3+} in biological and environmental systems, accurate Fe^{3+} quantification is essential for water quality assessment. Therefore, this research is interested in using reduced Schiff base ligand with simple synthesis and high yield. The specificity of this reduced Schiff base ligand as a sensor to determine the amount of Fe^{3+} in water samples with low lower limit of detection (LOD) and a linear coefficient (R^2) close to 1, make it a viable alternative for Fe^{3+} quantification in real water samples.

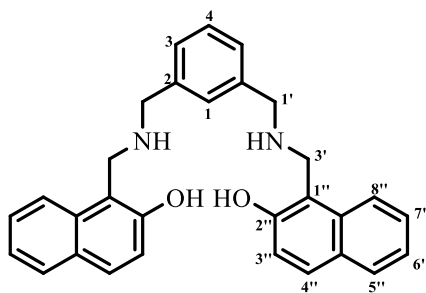


Figure 1 Structure of reduced Schiff base (RSB).

Materials and Methods

Chemicals and Equipment

A UV-visible spectrophotometer (model UV-2401PC, Shimadzu) was used to record absorption spectra and to measure absorbance. A nuclear magnetic resonance spectrometer (model Bruker Ascend 500, Bruker) was used at 500 MHz for ^1H -NMR, and at 125 MHz for ^{13}C -NMR. A mass spectrometer (model Dal-tonics (micro TOF), Bruker) was used to record mass spectra. Inductively coupled plasma optical emission spectroscopy (Perkin Elmer Avio 200) was used as a reference technique to compare the iron(III) content analysis results in the samples.

Salts of various types of heavy metal ions including $\text{Cd}(\text{ClO}_4)_2 \cdot \text{H}_2\text{O}$ (99.9%), $\text{Cu}(\text{ClO}_4)_2 \cdot 6\text{H}_2\text{O}$ (98%), $\text{Fe}(\text{ClO}_4)_2 \cdot \text{H}_2\text{O}$ (98%), $\text{Fe}(\text{ClO}_4)_3 \cdot \text{H}_2\text{O}$, $\text{Ni}(\text{ClO}_4)_2 \cdot 6\text{H}_2\text{O}$ (98%), $\text{Mn}(\text{ClO}_4)_2 \cdot 6\text{H}_2\text{O}$ (99%), $\text{Pb}(\text{ClO}_4)_2 \cdot 3\text{H}_2\text{O}$ (99%), $\text{Zn}(\text{ClO}_4)_2 \cdot 6\text{H}_2\text{O}$ (98%), AgNO_3 (99%), and HgCl_2 (98%) were purchased from Sigma Aldrich. NaCl (98%), KCl (98%), MgCl_2 (98%), and $\text{CrCl}_3 \cdot 6\text{H}_2\text{O}$ (95%) were purchased from UNILAB. All chemicals were AR grade.

Synthesis of reduced Schiff base

The synthesis of reduced Schiff base ligand has been reported from the research of Sungwienwong et al. [36], which is a simple synthesis method, using a mild reaction with high yield (84%). The structure of reduced Schiff base ligand was characterized by IR, $^1\text{H-NMR}$, $^{13}\text{C-NMR}$ and mass spectrometry. The results are as following: IR (ATR) ν_{max} 3293, 3055, 2851, 1621, 1597, 1514, 1467, 1437, 1357, 1327, 1267, 1235, 1130, 1089, 955, 904, 812, 744 cm^{-1} ; $^1\text{H-NMR}$ (500 MHz, DMSO d_6): δ 3.63 (4H, s, H-3'), 4.01 (4H, s, H-1'), 7.07 (2H, d, J = 8.8 Hz, H-3''), 7.10 (2H, t, J = 7.6 Hz, H-7''), 7.17–7.21 (5H, m, H-1, H-3, H-6''), 7.35 (1H, t, J = 7.4 Hz, H-4), 7.59 (2H, d, J = 8.5 Hz, H-8''), 7.65 (2H, d, J = 8.8 Hz, H-4''), 7.70 (2H, d, J = 8.0 Hz, H-5''); $^{13}\text{C-NMR}$ (125 MHz, DMSO d_6): δ 48.1 (C-1'), 58.1 (C-3'), 113.8 (C-9''), 118.0 (C-3''), 122.3 (C-6''), 122.7 (C-8''), 125.8 (C-7''), 128.0 (C-10''), 128.1 (C-5''), 128.6 (C-3), 129.0 (C-4''), 131.3 (C-1), 133.4 (C-1''), 137.7 (C-2), 154.5 (C-2''); HR-ESI-MS m/z 449.2231 $[\text{M} + \text{H}]^+$ (calculated for $\text{C}_{30}\text{H}_{29}\text{N}_2\text{O}_2$ 449.2223).

Study of the selective binding of reduced Schiff base ligand with various cations.

The solutions of metal cations; Na^+ , K^+ , Mg^{2+} , Mn^{2+} , Fe^{2+} , Co^{2+} , Ni^{2+} , Cu^{2+} , Zn^{2+} , Hg^{2+} , Cd^{2+} , Pb^{2+} , Cr^{3+} , Fe^{3+} (3.00×10^{-4} M) and the solution of reduced Schiff base (1.00×10^{-5} M) were prepared. The reduced Schiff base solution (2.00 mL) was mixed with each metal ion (2.00 mL). The absorbance of the mixtures was determined at 250-700 nm.

The solutions of metal cations; Na^+ , K^+ , Mg^{2+} , Mn^{2+} , Fe^{2+} , Co^{2+} , Ni^{2+} , Cu^{2+} , Zn^{2+} , Hg^{2+} , Cd^{2+} , Pb^{2+} , Cr^{3+} , Fe^{3+} (1.00×10^{-4} M) and the solution of reduced Schiff base (1.00×10^{-5} M) were prepared. The reduced Schiff base solution (1.00 mL) was mixed with each metal ion (1.00 mL). The absorbance of the mixtures was determined at 380 nm. Then, the solution of Fe^{3+} (1.00 mL) was added to the above mixture solution, and the absorbance of the solutions was determined at 380 nm. The absorbance in the absence and presence of Fe^{3+} was compared.

Binding study of reduced Schiff base with Fe^{3+}

The titration of reduced Schiff base ligand was performed by adding the Fe^{3+} solution (1.00×10^{-3} M) 50 μL -interval to the reduced Schiff base ligand (1.00×10^{-5} M, 2.00 mL) until the volume of Fe^{3+} solution was 800 μL . The absorption spectra were measured in the wavelength range of 300-700 nm, and the spectra of the reduced Schiff base ligand in the presence of each concentration of Fe^{3+} were compared.

The absorption spectra of standard Fe^{3+} solution with various concentrations, 3.00×10^{-6} , 1.00×10^{-4} , 2.00×10^{-4} , 3.00×10^{-4} , 5.00×10^{-4} and 1.00×10^{-3} M, were measured at 380 nm. Calibration curve of the absorbance versus standard Fe^{3+} concentration was constructed for LOD and LOQ determination.

The effect of pH on Fe^{3+} measurement with reduced Schiff base ligand.

The reduced Schiff base ligand (1.00×10^{-5} M) and Fe^{3+} (3.00×10^{-4} M) solutions were prepared at pH 3, 5, 9 and 12. The absorbance at 380 nm of reduced Schiff base ligand solution (2.00 mL) was measured in the absence and presence of standard Fe^{3+} solution (2.00 mL) for all pHs.

The interferent effect of various metal ions on Fe³⁺ measurement with reduced Schiff base ligand

The reduced Schiff base ligand (1.00×10^{-5} M, 2.00 mL) was mixed with Fe³⁺ solution (1.00×10^{-4} M, 1.00 mL). The absorbance at 380 nm of the mixture solution was measured. Then, the absorbance was measured with addition of other metal ions (3.00×10^{-4} M, 1.00 mL) to the above mixture.

Application of reduced Schiff base for quantitation of Fe³⁺ in water samples

Water sample solutions with Fe³⁺ concentrations of 1.0×10^{-4} M and 3.00×10^{-4} M in tap water, canal water, and drinking water were prepared by calculating the volume of Fe³⁺ solution used from the standard solution. Then, the volume was adjusted with tap water, canal water and drinking water. The reduced Schiff base ligand solution (1.00×10^{-5} M, 2.00 mL) was mixed with each type of water sample. The absorbance at a wavelength of 380 nm was measured, and used to determine the amount of Fe³⁺ from the standard calibration curve.

Results and Discussion

The synthesis of reduced Schiff base ligand has been reported in the research of Sungwienwong et al. [36] using the coupling reaction between 2-hydroxy-1-naphthadehyde and *m*-xylylene diamine to obtain Schiff base naphthalene-2-ol and reduced with sodium borohydride (NaBH₄) to obtain reduced Schiff base. The structure of reduced Schiff base was identified using NMR, IR and mass spectroscopic techniques.

The specificity study of the reduced Schiff base ligand in selective binding to various types of metal ions, including Fe³⁺, Cr³⁺, Pb²⁺, Co²⁺, Cu²⁺, Zn²⁺, Cd²⁺, Hg²⁺, Mn²⁺, Ni²⁺, Ag⁺, Na⁺, Mg²⁺, K⁺, Fe²⁺ showed only selectivity of Fe³⁺. New peaks in the range of 350-420 nm were observed with the significant change of the absorption spectrum of reduced Schiff base due to ligand-to-metal charge transfer (LMCT). However, other metal ions did not change the spectra of reduced Schiff base except Fe²⁺ and Cu²⁺, as shown in Figure 2. The reduced Schiff base ligand showed selective binding to Fe³⁺ as observed by the increase of the absorbance of reduced Schiff base ligand when Fe³⁺ was added, as shown in Figure 3.

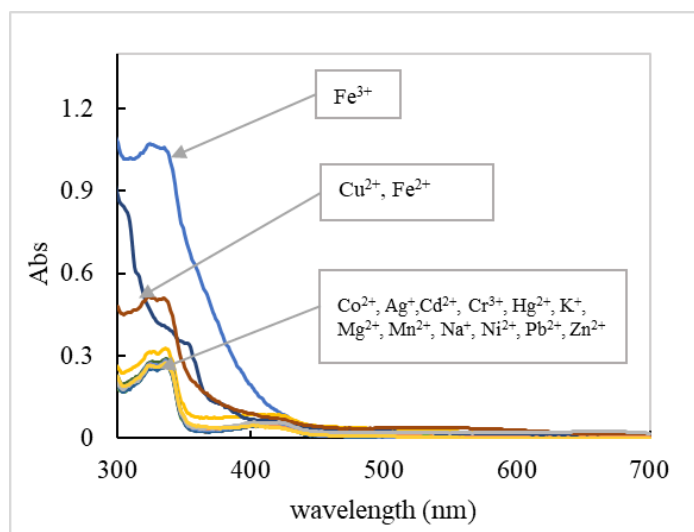


Figure 2 Absorption spectra of reduced Schiff base solution in the presence of various metal ions (3.0×10^{-4} M).

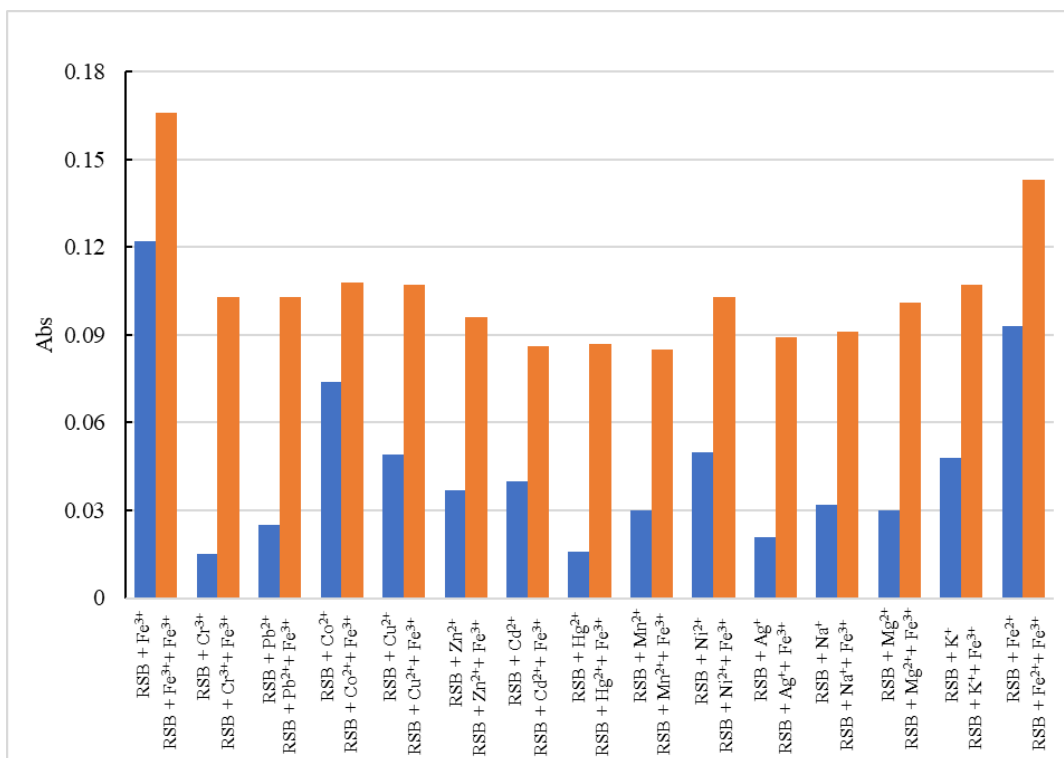


Figure 3 The bar graph shows the absorbance of RSB (1.00×10^{-5} M) with various metal ions (3.00×10^{-4} M) before adding (blue) and after adding 3.00×10^{-4} M of Fe^{3+} solution (orange) at 380 nm.

The binding efficiency of the reduced Schiff base ligand with Fe^{3+} was evaluated by monitoring absorbance changes upon Fe^{3+} addition. When Fe^{3+} was added to the reduced Schiff base ligand solution, the absorbance in the wavelength range of 350-420 nm increased with increasing volume of Fe^{3+} , as shown in Figure 4. The plot of absorbance value at a wavelength of 380 nm versus the concentration of Fe^{3+} added gave a straight line with a linear correlation coefficient (R^2) of 0.9974, as shown in Figure 5.

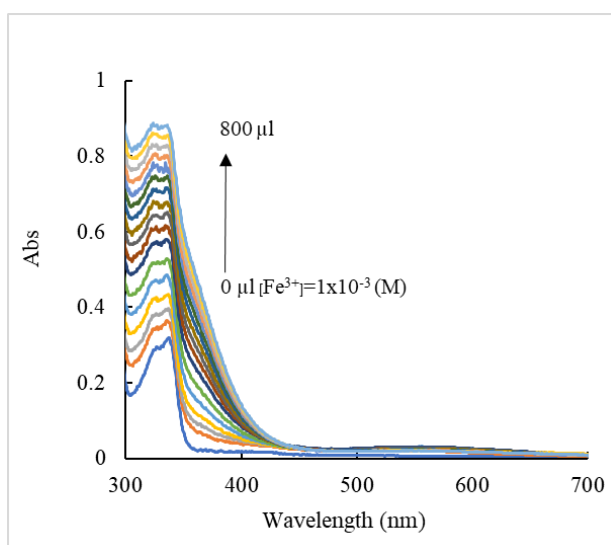


Figure 4 Absorption spectra of reduced Schiff base solution in the presence of 0.0-800.0 μL of 1.0×10^{-3} M Fe^{3+} .

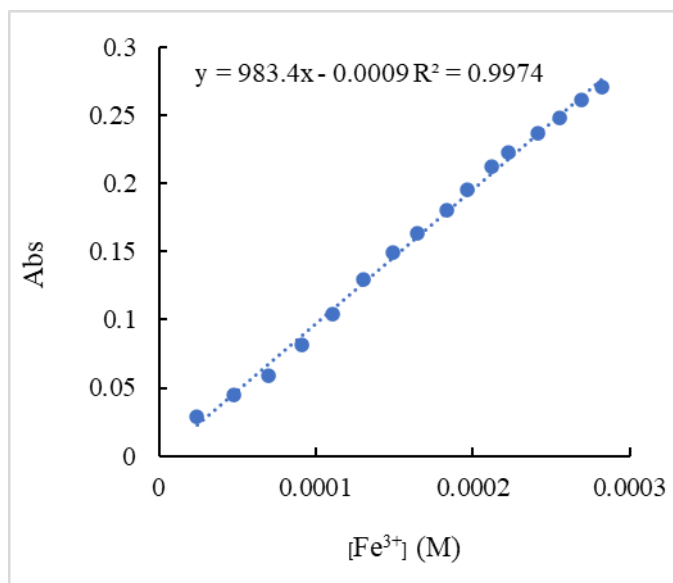


Figure 5 The linear relationship of absorbance versus Fe^{3+} concentration.

The linear relationship of the absorbance at 380 nm with the Fe^{3+} concentration with a linear correlation coefficient (R^2) of 0.9994 was confirmed by creating a standard curve. The limit of detection (LOD) and limit of quantification (LOQ) were calculated as three times and ten times the standard deviation (SD) of the blank solution signal measurements in 10 replicates. LOD and LOQ were found to be 1.22×10^{-6} M and 2.03×10^{-6} M, respectively, as shown in Figure 6.

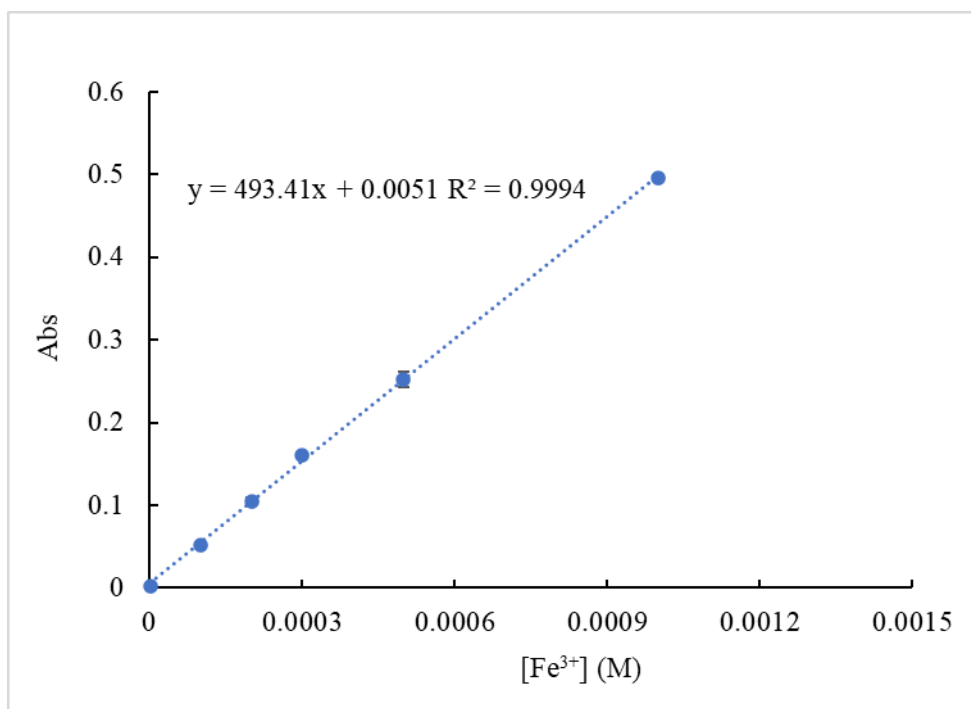


Figure 6 Standard graph showing a linear relationship between the absorbance at 380 nm and Fe^{3+} concentration in the range of 1.00×10^{-6} - 1.00×10^{-3} M when using the reduced Schiff ligand at a concentration of 1.00×10^{-5} M.

The results of the pH effect on the reduced Schiff base ligand solution in the range pH of 3–12 are shown in Figure 7. The spectra of the reduced Schiff base ligand at pH 3–12 did not change. Only at pH 3, the absorbance at the highest wavelength decreased due to the protonation of OH and NH functional groups of RSB. Comparison the spectra of reduced Schiff base ligand solution at the pH 3–12 before and after adding Fe^{3+} throughout the studied pH range, showed no effect of pH on Fe^{3+} binding, as shown in Figure 8.

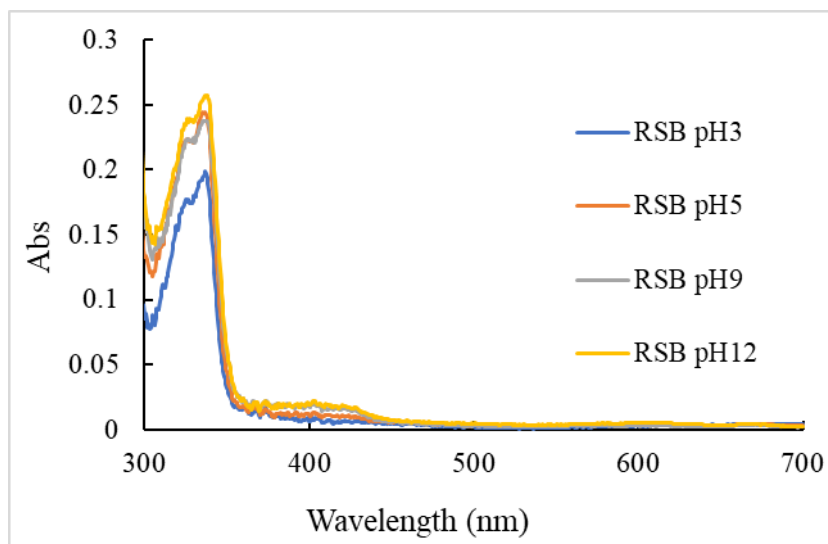


Figure 7 Absorption spectra of 1.00×10^{-5} M of RSB at pH 3, 5, 9 and 12.

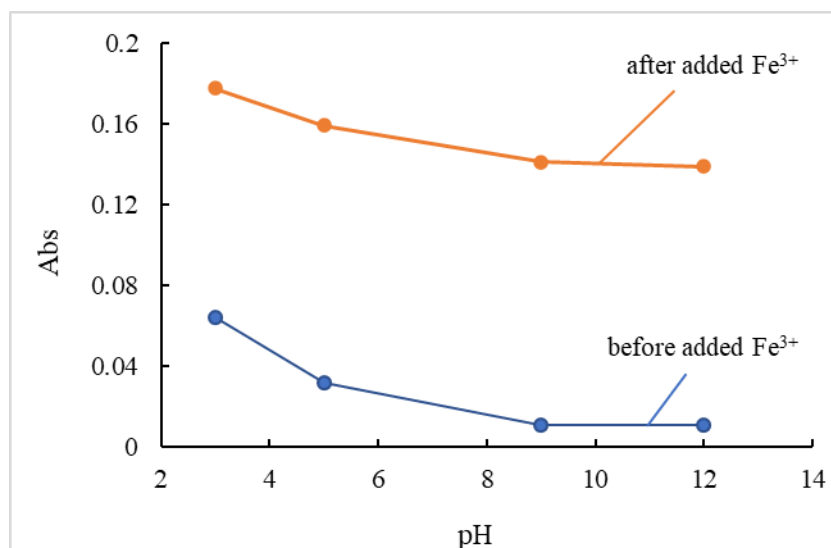


Figure 8 The absorbance of 1.00×10^{-5} M of RSB before and after adding 3.00×10^{-4} M of Fe^{3+} solution at pH 3-12 measured at 380 nm.

The interference effects of various types of ions to the quantitative analysis were studied by analyzing Fe^{3+} solutions at a concentration level of 1.00×10^{-4} M, and the absorbance at 380 nm was determined. Then, other metal ions (3.00×10^{-4} M) were added, and the absorbance was compared as shown in Figure 9. The results showed that the absorbance value when adding other metal ions changed by more than 5.00 %. Only Fe^{2+} had a change in absorbance of 12.94 %. However, determination of the amount of iron in water samples was the determination of the total amount of Fe^{3+} and Fe^{2+} and did not affect the analysis.

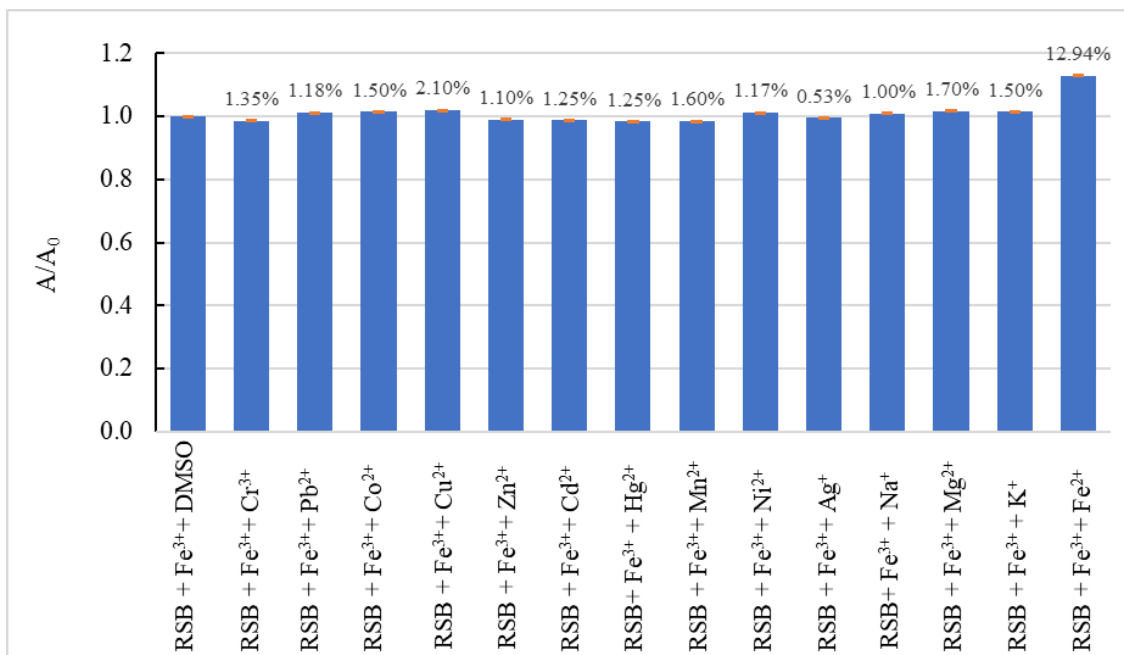


Figure 9 The changes in absorbance at 380 nm of the 2.00 mL RSB (1.00×10^{-5} M) mixed with 1.00 mL Fe^{3+} (1.00×10^{-4} M) in the presence of different types of 1.00 mL cations (3.00×10^{-4} M).

The reduced Schiff base ligand was applied as a sensor to quantify the amount of Fe^{3+} in real water samples from three sources; tap water, canal water and drinking water. Fe^{3+} solution with concentrations of 1.00×10^{-4} and 3.00×10^{-4} M were added to each water sample. Then, analysis was performed by mixing each type of water sample with reduced Schiff base ligand solution in a ratio of 1:1 by volume and the absorbance of the solutions was measured at 380 nm. The analysis results showed percentage recoveries ranging from 97.76% to 104.33%, with the measured Fe^{3+} concentrations differing from those obtained by the standard method only 1.51% to 2.70%, all within a 95% confidence interval, as shown in Table 1. The results indicated that the reduced Schiff base ligand was highly effective sensor for measuring the amount of Fe^{3+} in water samples, offering accuracy and reliability comparable to standard analytical methods.

Table 1 Quantity of Fe^{3+} in real water samples using the developed method (reduced Schiff base ligand) comparison with the standard method, Inductive coupled plasma optical emission spectroscopy (ICP), and the percentage recovery from the developed method.

Type of sample	Spiked $[\text{Fe}^{3+}]$ (M)	$[\text{Fe}^{3+}]$ found (M) (RSD, n=3)		%Recovery (RSD, n=3)	%Error
		Reduced Schiff base	ICP		
Tap water	1.00×10^{-4}	$0.99 \pm 0.160 \times 10^{-4}$ (1.62)	$1.01 \pm 0.007 \times 10^{-4}$ (0.70)	98.80 ± 1.60	2.19
	3.00×10^{-4}	$3.04 \pm 0.044 \times 10^{-4}$ (1.45)	$2.96 \pm 0.02 \times 10^{-4}$ (0.68)	101.33 ± 0.47	2.70
Drinking water	1.00×10^{-4}	$0.98 \pm 0.160 \times 10^{-4}$ (1.63)	$0.99 \pm 0.06 \times 10^{-4}$ (0.60)	98.40 ± 1.60	1.28
	3.00×10^{-4}	$3.13 \pm 0.046 \times 10^{-4}$ (1.47)	$3.05 \pm 0.025 \times 10^{-4}$ (0.82)	104.33 ± 1.47	2.63
Canal water	1.00×10^{-4}	$0.98 \pm 0.18 \times 10^{-4}$ (1.84)	$0.99 \pm 0.05 \times 10^{-4}$ (0.50)	97.90 ± 1.80	1.51
	3.00×10^{-4}	$2.93 \pm 0.018 \times 10^{-4}$ (0.61)	$2.87 \pm 0.015 \times 10^{-4}$ (0.52)	97.76 ± 0.60	2.09

Comparing the results of the reduced Schiff base ligand with previous works on Fe^{3+} measurement showed that the reduced Schiff base ligand provided a wide measurement range and a lower LOD value than those obtained from many researches, as shown in Table 2. The measurement of 2-1000 μM and LOD of 1.22 μM were obtained from this study. Moreover, the developed method can be used to quantify Fe^{3+} in real water samples. Therefore, the reduced Schiff base ligand has potential as a sensor for detecting Fe^{3+} in natural water sources.

Table 2 Comparison of efficiency of different sensors for detection of Fe^{3+}

Type of probe	Mechanism	Linear range (μM)	LOD (μM)	References
Gold nanoparticles	Aggregation	10–60	5.60	[37]
Metal organic framework (MIL-53)	Ions exchange	3-200	9.00	[38]
Graphene quantum dots	Coordination	0-400	7.22	[39]
Silver nanoparticles	Reduction	0.08-80	0.08	[40]
Chromophore	Coordination	0-100	5.37	[41]
Silver nanoparticles	Coordination	9- 9000	7.90	[42]
Silver nanoparticles	Coordination	7-1790	1.79	[43]
Chromophore	Coordination	2-1000	1.22	This work

Conclusions

The binding interaction between the reduced Schiff base ligand and Fe^{3+} was analyzed by UV-visible spectrophotometry. New peaks in the wavelength range of 350-400 nm were detected due to ligand-to-metal charge transfer (LMCT) upon complex formation. The absorbance of the complex at 380 nm has a linear correlation with the amount of added Fe^{3+} . In this study, the reduced Schiff base ligand can be applied as a sensor for analyzing the amount of Fe^{3+} in real water samples. The developed analytical method gave a linear standard curve in the concentration range from 2.00×10^{-6} – 1.00×10^{-3} M with LOD and LOQ of 1.22×10^{-6} and 2.03×10^{-6} M, respectively. This method showed analytical results similar to those obtained from standard techniques. Therefore, this method offers a cost-effective, rapid, and straightforward approach for Fe^{3+} quantification in real water samples, requiring minimal reagent quantities.

Acknowledgements

The authors would like to thank Faculty of Science, Srinakharinwirot University for the supporting research tools and facilities. Scholarship for student from the collaboration with Thailand International Cooperation Agency (TICA) is gradually acknowledged.

References

1. Abbaspour N, Hurrell R, Kelishadi R. Review on iron and its importance for human health. *J Res Med Sci.* 2014;19(2):164-74.
2. Ali MK, Kim RY, Karim R, Mayall JR, Martin KL, Shahandeh A, et al. Role of iron in the pathogenesis of respiratory disease. *Int J Biochem Cell Biol.* 2017;88:181-95.
3. Cheng R, Dhorajia VV, Kim J, Kim Y. Mitochondrial iron metabolism and neurodegenerative diseases. *Neurotoxicology.* 2022;88:88-101.
4. Rishi G, Subramaniam VN. Biology of the iron efflux transporter, ferroportin. *Adv Protein Chem Struct Biol.* 2021;123:1-16.
5. Wu Q, Wei C, Guo S, Liu J, Xiao H, Wu S, et al. Acute iron overload aggravates blood-brain barrier disruption and hemorrhagic transformation after transient focal ischemia in rats with hyperglycemia. *IBRO Neurosci Rep.* 2022;13:87-95.
6. Baschant U, Altamura S, Steele-Perkins P, Muckenthaler MU, Spasić MV, Hofbauer LC, et al. Iron effects versus metabolic alterations in hereditary hemochromatosis driven bone loss. *Trends Endocrinol Metab.* 2022;33(9):652-63.
7. Liu S, Cao X, Wang D, Zhu H. Iron metabolism: state of the art in hypoxic cancer cell biology. *Arch Biochem Biophys.* 2022;723:109199.
8. Rishi G, Huang G, Subramaniam VN. Cancer: the role of iron and ferroptosis. *Int J Biochem Cell Biol.* 2021;141:106094.
9. Higashida K, Inoue S, Nakai N. Iron deficiency attenuates protein synthesis stimulated by branched-chain amino acids and insulin in myotubes. *Biochem Biophys Res Commun.* 2020;531(2):112-7.

10. Dai Y, Liu X, Wang P, Fu J, Yao K, Xu K. A new fluorescent probe based on quinoline for detection of Al^{3+} and Fe^{3+} with “off-on-off” response in aqueous solution. *RSC adv.* 2016;6(102):99933-9.
11. Wang L, Yang L, Cao D. A visual and fluorometric probe for Al(III) and Fe(III) using diketopyrrolopyrrole-based Schiff base. *Sens Actuators B: Chem.* 2014;202:949-58.
12. Freelandgraves JH, Sachdev PK, Binderberger AZ, Sosanya ME. Global diversity of dietary intakes and standards for zinc, iron, and copper. *J Trace Elem Med Biol.* 2020;61:126515.
13. Zachariou V, Bauer CE, Seago ER, Panayiotou G, Hall ED, Butterfield DA, et al. Healthy dietary intake moderates the effects of age on brain iron concentration and working memory performance. *Neurobiol Aging.* 2021;106:183-96.
14. Asmari M, Abdel-Megied AM, Michalcová L, Glatz Z, El Deeb S. Analytical approaches for the determination of deferiprone and its iron(III) complex: investigation of binding affinity based on liquid chromatography-mass spectrometry (LC-ESI/MS) and capillary electrophoresis-frontal analysis (CE/FA). *Microchem J.* 2020;154:104556.
15. Pattaweepaiboon S, Foytong W, Phiomphu N, Nanok T, Kaewchangwat N, Suttisintong K, et al. Spirooxazine-based dual-sensing probe for colorimetric detection of Cu^{2+} and Fe^{3+} and its application in drinking water and rice quality monitoring. *ACS omega.* 2022;7(22):18671-80.
16. Sun Y, Jia Y, Han W, Sun Y, Wang J, Deng Z, et al. A highly selective and sensitive coumarin-based chemosensor for recognition of Al^{3+} and the continuous identification of Fe^{3+} in water-bearing system and biomaging & biosensing in Zebrafish. *J Mol Struct.* 2023;1284:135459.
17. Zhang S, Liu C, Yuan Y, Fan M, Zhang D, Wang D, et al. Selective, highly efficient extraction of Cr(III), Pb (II) and Fe (III) from complex water environment with a tea residue derived porous gel adsorbent. *Bioresour Technol.* 2020;311:123520.
18. Chen G, Lan H, Cai S, Sun B, Li X, He Z, et al. Stable hydrazone-linked covalent organic frameworks containing O, N, O-chelating sites for Fe (III) detection in water. *ACS Appl Mat Interfaces.* 2019;11(13):12830-7.
19. Mohamed KN, Gledhill M. Determination of specific iron chelator by using LC-ICP-MS and LC-ESI-MS. *Procedia Environ Sci.* 2015;30:256-61.
20. Wu D, Sedgwick AC, Gunnlaugsson T, Akkaya EU, Yoon J, James TD. Fluorescent chemosensors: the past, present and future. *Chem Soc Rev.* 2017;46(23):7105-23.
21. Li W, Wang L, Tang H, Cao D. Diketopyrrolopyrrole-based fluorescent probes for detection and bioimaging: current progresses and perspectives. *Dyes Pigm.* 2019;162:934-50.
22. Balamurugan R, Liu J, Liu B. A review of recent developments in fluorescent sensors for the selective detection of palladium ions. *Coord Chem Rev.* 2018;376:196-224.
23. Gupta VK, Singh AK, Kumawat LK. Thiazole Schiff base turn-on fluorescent chemosensor for Al^{3+} ion. *Sens Actuators B: Chem.* 2014;195:98-108.
24. Gupta VK, Singh AK, Kumawat LK. A turn-on fluorescent chemosensor for Zn^{2+} ions based on antipyrine schiff base. *Sens Actuators B: Chem.* 2014;204:507-14.
25. Fang H, Huang P, Wu F. A highly sensitive fluorescent probe with different responses to Cu^{2+} and Zn^{2+} . *Spectrochim Acta A: Mol Biomol Spectrosc.* 2019;214:233-8.

26. Song H, Zhang Z. A quinoline-based ratiometric fluorescent probe for discriminative detection of Zn^{2+} and Cd^{2+} with different binding modes, and its Zn^{2+} complex for relay sensing of pyrophosphate and adenosine triphosphate. *Dyes Pigm.* 2019;165:172-81.
27. Mironenko AY, Tutov M, Chepak A, Zadorozhny P, Bratskaya SY. A novel rhodamine-based turn-on probe for fluorescent detection of Au^{3+} and colorimetric detection of Cu^{2+} . *Tetrahedron.* 2019;75(11):1492-6.
28. Li Y, Niu Q, Wei T, Li T. Novel thiophene-based colorimetric and fluorescent turn-on sensor for highly sensitive and selective simultaneous detection of Al^{3+} and Zn^{2+} in water and food samples and its application in bioimaging. *Anal Chim Acta.* 2019;1049:196-212.
29. Zhang M, Gong L, Sun C, Li W, Chang Z, Qi D. A new fluorescent-colorimetric chemosensor based on a Schiff base for detecting Cr^{3+} , Cu^{2+} , Fe^{3+} and Al^{3+} ions. *Spectrochim Acta A: Mol Biomol Spectrosc.* 2019;214:7-13.
30. Liu J, Zheng Q, Yang J, Chen C, Huang Z. A new fluorescent chemosensor for Fe^{3+} and Cu^{2+} based on calix [4] arene. *Tetrahedron Lett.* 2002;43(50):9209-12.
31. Li N, Xu Q, Xia X, Lu J, Wen X. A polymeric chemosensor for Fe^{3+} based on fluorescence quenching of polymer with quinoline derivative in the side chain. *Materials Chemistry and Physics.* 2009;114(1):339-43.
32. Li Z, Zhang L, Zhao W, Li X, Guo Y, Yu M, et al. Fluoranthene-based pyridine as fluorescent chemosensor for Fe^{3+} . *Inorganic Chem Comm.* 2011;14(10):1656-8.
33. Li Z, Zhou Y, Yin K, Yu Z, Li Y, Ren J. A new fluorescence "turn-on" type chemosensor for Fe^{3+} based on naphthalimide and coumarin. *Dyes Pigm.* 2014;105:7-11.
34. Wang R, Wan Q, Feng F, Bai Y. A novel coumarin-based fluorescence chemosensor for Fe^{3+} . *Chem Res Chin Univ.* 2014;30(4):560-5.
35. Aussawaponpaisan P, Nusuwan P, Tongraung P, Jittangprasert P, Pumsa-ard K, Kuno M. Fluorescent Chemosensor for Cu^{2+} based on Schiff base-naphthalene-2-ol. *Mater Today: Proc.* 2017;4(5):6022-30.
36. Sungwienwong I, Tongraung P, Boonsri P, Apiratikul N. Reduced Schiff base as novel two-faced sensor for the detection of iron (III) and carbonate ions. *J Mol Struct.* 2024;1308:138126.
37. Wu S, Chen Y, Sung Y. Colorimetric detection of Fe^{3+} ions using pyrophosphate functionalized gold nanoparticles. *Analyst.* 2011;136(9):1887-91.
38. Yang C, Ren H, Yan X. Fluorescent metal-organic framework MIL-53 (Al) for highly selective and sensitive detection of Fe^{3+} in aqueous solution. *Anal Chem.* 2013;85(15):7441-6.
39. Ananthanarayanan A, Wang X, Routh P, Sana B, Lim S, Kim D, et al. Facile synthesis of graphene quantum dots from 3D graphene and their application for Fe^{3+} sensing. *Adv Funct Mater.* 2014;24(20):3021-6.
40. Gao X, Lu Y, He S, Li X, Chen W. Colorimetric detection of iron ions (III) based on the highly sensitive plasmonic response of the N-acetyl-l-cysteine-stabilized silver nanoparticles. *Anal Chim Acta.* 2015;879:118-25.
41. Liu X, Li N, Xu M-M, Wang J, Jiang C, Song G, et al. Specific colorimetric detection of Fe^{3+} ions in aqueous solution by squaraine-based chemosensor. *RSC adv.* 2018;8(61):34860-6.

42. Samerjai W, Jittangprasert P, Tongraung P. Colorimetric detection of iron (III) ion based on 4-aminothiophenol and schiff base naphthalene-2-ol modified silver nanoparticles. *Asian J Chem.* 2020;32(2):287-92.
43. Jittangprasert. P, Kerdkok D, Tongraung, P. Synthesis and application of novel modified silver nanoparticles for determination of iron (III) in wastewater. *J Res Unit Sci Tech Environ Learning.* 2020;11(2):316-31. (in Thai)